

# Kinetics and Mechanism for the Formation of b- and y-type Ions from Singly Protonated Peptides on a Microsecond Time Scale: The Arginine Mystery

Yeon Ji Chung, So Hee Yoon, and Myung Soo Kim\*

Department of Chemistry, Seoul National University, Seoul 151-742, Korea. \*E-mail:myungsoo@snu.ac.kr

Received August 9, 2008

A kinetic model was built for the formation of b and y ions – which are the main product ions generated from singly protonated peptides at low internal energy regime – on a microsecond time scale based on the potential energy diagram along the oxazolone pathway reported previously. The rate constants were evaluated using the Rice-Ramsperger-Kassel-Marcus theory. Even though migration of the extra proton to an amide nitrogen is a prerequisite in the oxazolone mechanism, it was found highly unlikely when this proton was sequestered at an arginine side chain. Possibility of migration of a proton from other locations such as a carboxyl group is discussed.

**Key Words :** Oxazolone pathway, b-y Ions, RRKM, Arginine

## Introduction

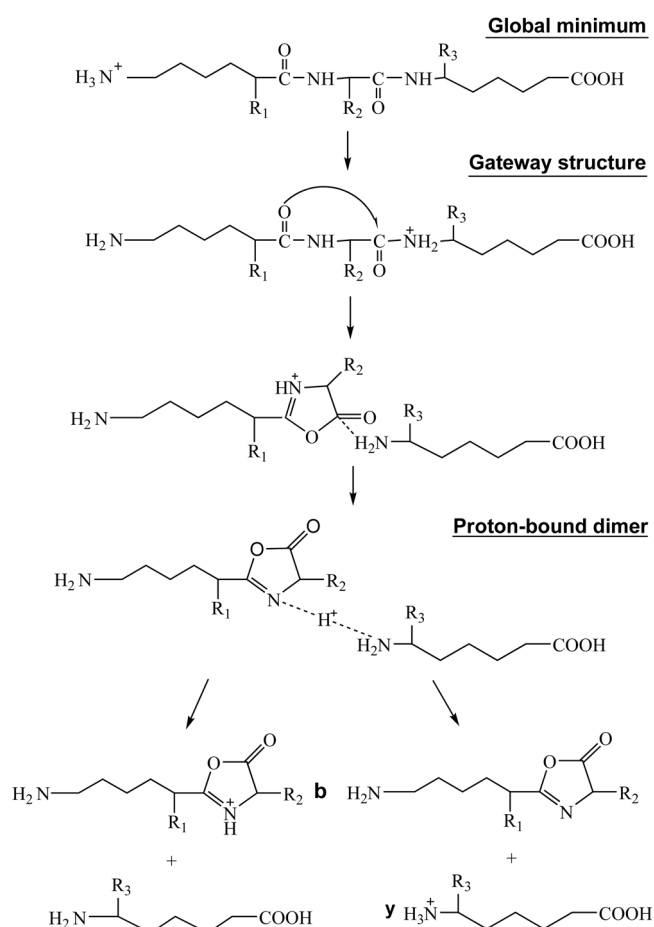
Tandem mass spectrometry is a widely used technique for protein identification and sequencing.<sup>1-4</sup> A standard procedure in the use of this technique is to produce small peptides from a protein by enzymatic digestion<sup>5</sup> and to record and analyze their tandem mass spectra. Trypsin is generally used for this purpose, which produces peptides – so-called tryptic peptides – with an arginine or lysine residue at the C-terminus. Accordingly, understanding the dissociation mechanism for protonated tryptic peptides – especially those with an arginine residue – is one of the important subjects in mass spectrometric analysis of proteins.

Dissociation of protonated peptides generated by techniques such as electrospray ionization (ESI)<sup>6</sup> and matrix-assisted laser desorption ionization (MALDI)<sup>7</sup> has been investigated extensively by various experimental and theoretical methods. When the internal energy of a protonated peptide generated by the above techniques is not large, charge-directed reactions are thought to be responsible for its dissociation, generating b- and y-type product ions. Two important outcomes – which are relevant to the present work – from the previous studies are the formulation of the ‘mobile proton model’<sup>8,9</sup> and the theoretical identification<sup>10-13</sup> of the reaction paths leading to the above product ions. In the mobile proton model, protons added in the formation of protonated peptides are classified into two groups, those that can migrate easily (mobile) along the peptide backbone and those that can not (localized). Specifically, a proton attached to an arginine residue – arginine is the most basic amino acid – is thought to be sequestered by the side chain and hence is difficult to migrate. In contrast, those attached to other basic sites such as the amino group at the N-terminus are assumed to migrate easily to amide nitrogens where charge-directed reactions are thought to occur. Primary evidences for the mobile proton model were found from the fragmentation efficiency data.<sup>8</sup> For example, dissociation of singly protonated peptides with one arginine

residue (no mobile proton) was found to require larger amount of internal energy than that of doubly protonated peptides (one mobile proton). However, it is not clear whether the extra proton sequestered at an arginine side chain can migrate, even though with some difficulty, or can not migrate at all.

Theoretical investigations on the formation of b- and y-type product ions have been focused on the dissociation of singly protonated species of simple peptides such as the trimer and pentamer of glycine and alanine.<sup>10-13</sup> Among various pathways proposed in the early phase of the study,<sup>13,14</sup> the oxazolone pathway is thought to be the most important at the moment.<sup>12,13</sup> A brief summary of the oxazolone pathway investigated by Paizs *et al.*<sup>11,13</sup> and by Siu *et al.*<sup>10</sup> at the density functional theory (DFT) level is shown in Scheme 1. In the structure corresponding to the global energy minimum, the extra proton is located at the amino group at the N-terminus. This migrates to the nitrogen atom of an amide bond, generating a reactive intermediate. Then, the cleavage of the protonated amide bond and subsequent intramolecular rotation results in a proton-bound dimer of an oxazolone derivative and a smaller peptide. Depending on the proton affinities of the oxazolone derivative and the peptide, proton can be retained in the former or latter moieties, generating either b- or y-type ions, respectively. It is to be noted that the extra proton is assumed to be initially attached to the amino group at the N-terminus in the calculation, *viz.* it is treated as a mobile proton. It is well known<sup>15</sup> that tandem mass spectra recorded under low internal energy regime are dominated by b- and/or y-type product ions even when an arginine residue is present in singly protonated peptides, *viz.* when the extra proton is not thought to be mobile. It is not known, however, whether the oxazolone pathway is also applicable in the presence of arginine.

As a part of our study on the time-resolved ultraviolet photodissociation (UV-PD)<sup>16,17</sup> of singly protonated peptides with an arginine residue at the N-terminus, rough estimations for statistical – Rice-Ramsperger-Kassel-Marcus



**Scheme 1.** Oxazolone pathway for the formation of b- and y-type ions from a singly protonated peptide without an arginine residue

(RRKM)<sup>18-20</sup> – rate constants were made for the dissociation of a singly protonated peptide. It had to be postulated in the work that the critical energy for the production of b-type ions in the presence of arginine was only slightly – by a few tenths of an eV – larger than that in its absence. This was a surprising result in view of the dichotomy, ‘mobile’ *vs.* ‘localized’ protons, used in the mobile proton model. This paper presents the results from further computational kinetic studies made to highlight the difficulties in applying the above models to the dissociation of singly protonated peptides with an arginine residue and to probe their mechanistic implication.

### Computation

The rate-energy relation,  $k(E)$ , was calculated using the following RRKM expression.<sup>18-20</sup>

$$k(E) = \sigma \frac{N^\ddagger(E - E_0)}{h\rho(E)} \quad (1)$$

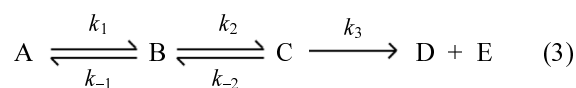
Here  $\rho(E)$  is the vibrational state density of the reactant at the internal energy  $E$ ,  $E_0$  is the critical energy of the reaction,  $N^\ddagger(E - E_0)$  is the vibrational state sum from 0 to  $E - E_0$  at the transition state (TS),  $h$  is the Planck constant and  $\sigma$  is the

reaction path degeneracy which is usually one for reactions involving large molecules. Details of the method and the software used to calculate  $k(E)$  for the dissociation of singly protonated peptides were reported previously.<sup>21-23</sup> The vibrational frequency set for a singly protonated peptide, which is needed to evaluate  $\rho(E)$ , is automatically generated by the software once the amino acid sequence of the peptide is supplied. The frequency set at TS, which is needed to evaluate  $N^\ddagger(E - E_0)$ , is also generated automatically once the entropy of activation,  $\Delta S^\ddagger$ ,<sup>24,25</sup> at 1000 K is designated. The software deletes the frequency of the vibration along the reaction coordinate (taken as 1149  $\text{cm}^{-1}$ ) and adjusts six low-frequency vibrations such that the designated  $\Delta S^\ddagger$  results.  $\Delta S^\ddagger = 0$  eu (1eu = 4.184  $\text{J K}^{-1} \text{mol}^{-1}$ ) was assumed for the formation of b- and y-type ions, which is thought to occur *via* tight transition state. The Beyer-Swinehart algorithm<sup>26</sup> was used to calculate the state sum and density with the grain size of 1  $\text{cm}^{-1}$ . The same software also calculates the internal energy distribution,  $P(E)$ , for a singly protonated peptide at a specified temperature using the following equation.

$$P(E) \propto \rho(E)\exp(-E/kT) \quad (2)$$

### Results and Discussion

**Potential energy along the reaction path and the kinetic model.** According to the DFT results reported by Paizs *et al.*<sup>11,12</sup> and by Siu *et al.*,<sup>10</sup> the oxazolone pathways for the formation of b- and y-type ions consist of many steps involving isomerization, tautomerization, and bond breaking. To estimate the overall rate constant,  $k$ , for a particular dissociation channel, we do not have to take into account all these steps as will become clear later. Let us consider the kinetic scheme in eqn. (3) – interconversion between the global minimum structure (A) and the structure with the extra proton at an amide nitrogen (B), cleavage of the protonated amide bond in B to form a proton-bound dimer (C), and separation of C into the final products (D + E). The transition structure in each step will be denoted as  $\text{TS}_{\text{AB}}$ ,  $\text{TS}_{\text{BC}}$ , and  $\text{TS}_{\text{CD}}$ , respectively.



The potential energies of B, C, D + E, and  $\text{TS}_{\text{BC}}$  relative to that of A were calculated at the DFT level by Paizs and Suhai<sup>12</sup> for the b<sub>2</sub>-y<sub>3</sub>, b<sub>3</sub>-y<sub>2</sub>, and b<sub>4</sub>-y<sub>1</sub> oxazolone channels of the singly protonated alanine pentamer ([AAAAA + H]<sup>+</sup>). Values close to the averages over the three channels have been used to draw the schematic potential energy diagram shown in Figure 1. Even though the potential energy at  $\text{TS}_{\text{AB}}$  was not reported in the above reference, it is thought to be lower than that at  $\text{TS}_{\text{BC}}$  according to the results for smaller singly protonated peptides.<sup>11</sup> The potential energy at  $\text{TS}_{\text{CD}}$  should be very close to that at D + E because the separation of the proton-bound dimer is thought to occur without a significant reverse barrier.<sup>14</sup>

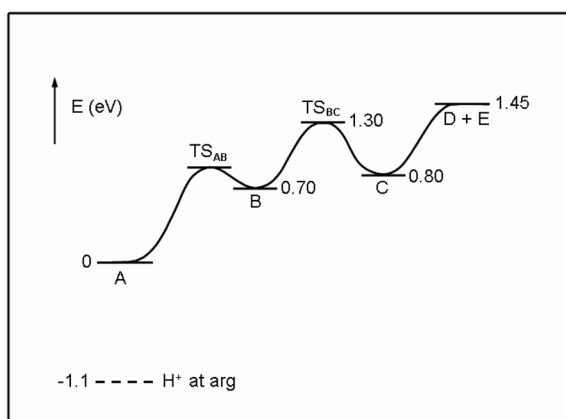
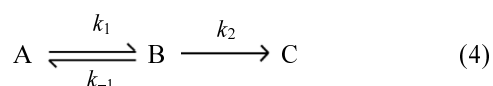


**Figure 1.** Potential energy diagram for the formation of b- and y-type product ions from a singly protonated peptide. A is the structure at the global minimum, B is the structure with the extra proton at an amide nitrogen, C is the proton-bound dimer, and D + E are the products. In the absence of an arginine residue, the extra proton is attached to the N-terminus amino group in the global minimum.  $TS_{AB}$  and  $TS_{BC}$  represent transition structures between A and B and between B and C, respectively. Numbers are relative potential energies, in eV, for each structure estimated from a previous DFT study<sup>11</sup> on  $[AAAAA+H]^+$ . Potential energy at the global minimum decreases when an arginine residue is present, shown as a dashed line.

It will be shown later that most of the singly protonated peptides at C (proton-bound dimer) dissociate to D and E, *viz.*  $k_3 \gg k_{-2}$ , when their internal energies are large enough for dissociation on the experimental time scale of 1-20  $\mu$ sec for post-source decay (PSD) in the tandem time-of-flight mass spectrometer in the authors' laboratory. This further simplifies the kinetic scheme into eqn. (4).



This corresponds to a well-known case of unimolecular dissociation after isomerization.<sup>27</sup> As mentioned above, it is likely that  $B \rightarrow C$  occurs *via* higher energy barrier than  $B \rightarrow A$  or to the structure with the extra proton at the amide oxygen. On the other hand,  $\Delta S^\ddagger$  for the former reaction which occurs *via* a 5-membered ring transition state<sup>11</sup> will be smaller than that for the latter reaction(s) that involves proton migration. Hence, it is highly likely that  $k_2 \ll k_{-1}$ . Then, the rate constant,  $k$ , for  $A \rightarrow C$  is well approximated by  $k_1 k_2 / k_{-1}$ , resulting in the following RRKM expression.

$$k(E) = \sigma \frac{N^\ddagger(TS_{BC})}{h \rho(A)} \quad (5)$$

The symbols inside the parantheses indicate that the state density  $\rho$  must be evaluated at the global minimum (A) while  $N^\ddagger$  is evaluated at  $TS_{BC}$ . It is to be noted that participation of other isomerization/tautomerization steps occurring *via* TSs at lower energies than that of  $TS_{BC}$  would not affect the rate constant in the above kinetic scheme and hence can be ignored, as has been mentioned already.

Even if the potential energy diagram in Figure 1 is valid,

eqn. (5) is not a good estimate for the overall rate constant when  $k_3 \gg k_{-2}$  does not hold. When the reaction occurs at the threshold,  $C \rightarrow D + E$  can be rate-determining<sup>28</sup> and, following the same argument as above,  $N^\ddagger(TS_{BC})$  in eqn. (5) may have to be replaced by  $N^\ddagger(TS_{CD})$ . Then, as the internal energy increases, the rate-determining TS will change from  $TS_{CD}$  (a loose TS with positive  $\Delta S^\ddagger$ ) to  $TS_{BC}$  (a tight TS with zero or negative  $\Delta S^\ddagger$ ), a case of TS switching. That is, the kinetic model for reactions occurring on nanosecond-to-microsecond time scale dealt with in this work can be different from that occurring on millisecond-to-second time scale.

**$k(E)$  for oxazolone pathway and  $P(E)$ .** In our previous work,<sup>17</sup> PSD and UV-PD spectra for several singly protonated peptides with an arginine residue generated by MALDI were compared. Some aspects of the UV-PD spectral patterns – such as that the observed product ion types were the same regardless of the chromophore excited – strongly suggested statistical dissociation of photoexcited singly protonated peptides. In the PSD spectra,  $b_n$  ions and their consecutive reaction products appeared dominantly. In UV-PD spectra, they got weaker and gave way to  $a_n$  and  $d_n$  ions. According to a previous report,<sup>29</sup> the latter ions are consecutively formed from  $a_n + 1$  ions which, in turn, are formed from singly protonated peptides *via* simple bond cleavage. That is, the overall situation looked like a textbook case of the competition between reactions occurring *via* tight TS ( $b_n$ , small  $E_0$  and small  $\Delta S^\ddagger$ ) and those *via* loose TS ( $a_n + 1$ , large  $E_0$  and large  $\Delta S^\ddagger$ ). We also investigated the time evolution of each product ion signal by using the time-resolved UV-PD technique developed previously,<sup>16</sup> which can separate product ions formed within 100 nsec (fast component) after photoexcitation and those between 0.2 and 5  $\mu$ sec (slow component). It was found that ions formed *via*  $b_n$  channels had both fast and slow components while those *via*  $a_n + 1$  channels had fast components mostly. Such an apparently nonstatistical behavior was accommodated within the statistical picture by taking into account the fact that protonated peptides generated by MALDI had broad internal energy distributions ( $P(E)$ ). Then, we attempted to explain all the observed temporal features based on the RRKM rate-energy relations ( $k(E)$ ) and  $P(E)$ . Protonated peptides in MALDI plume were assumed to be at an effective temperature  $T$  and  $P(E)$  was calculated at this temperature using eqn. (2). The same kinetic parameters –  $E_0$  and  $\Delta S^\ddagger$  – were assumed for generation of the same type product ions. By adjusting  $E_0$ ,  $\Delta S^\ddagger$ , and  $T$ , we could obtain  $k(E)$  and  $P(E)$  which were qualitatively compatible with the temporal characteristics of the PSD and time-resolved UV-PD data. In the case of  $\Delta S^\ddagger$  for the formation of  $b_n$  ions, zero or negative values (in eu unit) were found to be adequate, in agreement with our postulation that this type of ions are formed *via* tight TS. Qualitatively reasonable results could be obtained by simultaneously increasing or decreasing  $E_0$  and  $T$  values. That is,  $E_0$  for the formation of  $b_n$  ions could not be determined uniquely. We used  $k(E)$  calculated with  $E_0 = 1.4$  eV and  $\Delta S^\ddagger = 0$  eu for the formation of  $b_n$  ions from singly

protonated substance  $P$ ,  $[\text{RPKPQQFFGLM-NH}_2+\text{H}]^+$ , and  $P(E)$  calculated at 700 K to explain its PSD and time-resolved UV-PD results. We also showed that  $E_0$  had to be slightly lowered, say to 1.28 eV, when  $\Delta S^\ddagger$  was kept at 0 eu if the arginine effect – further stabilization of the extra proton by arginine residue – had been absent. It is to be mentioned that  $E_0$  of 1.28 eV and  $\Delta S^\ddagger$  of 0 eu are close to the DFT result of 1.275 eV and  $-1.0$  eu, respectively, for  $[\text{AGG} + \text{H}]^+$  reported by Bythell *et al.*<sup>30</sup>

In this work, we repeated a similar calculation, but for  $[\text{PKPQQFFGLMR}+\text{H}]^+$ . The reason for using this cation as the test case will become clear later.  $\Delta S^\ddagger = 0$  eu was used as before while  $E_0 = 1.30$  eV in Figure 1 was used as if the arginine residue had been absent.  $k(E)$  thus obtained is shown in Figure 2(a).  $k(E)$  calculated for the singly protonated substance  $P$  is essentially the same as far as the same values of the kinetic parameters are used. The experimental  $k$  range estimated from the PSD time scale was  $4 \times 10^4 - 7 \times 10^5 \text{ sec}^{-1}$ . Assuming that 10 such channels compete, this range was lowered by the factor of 10 and is drawn in Figure 2(a). To estimate the internal energy range for the protonated peptides generated by MALDI,  $P(E)$  was calculated at 700

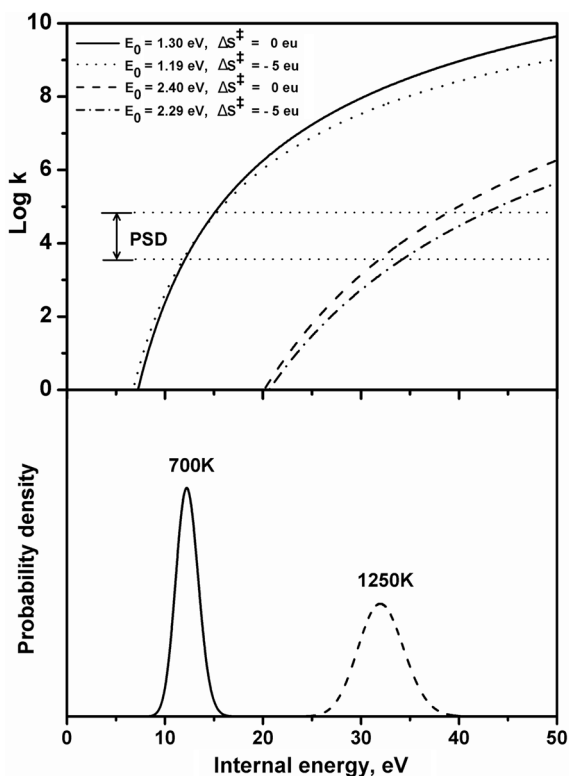


**Figure 2.** (a) The RRKM rate-energy curves,  $k(E)$ , for  $[\text{PKPQQFFGLMR}+\text{H}]^+$  calculated with the kinetic parameters ( $E_0$  in eV,  $\Delta S^\ddagger$  in eu) of (1.3, 0.0, solid line), (1.19,  $-5.0$ , dotted line), (2.4, 0.0, dashed line), and (2.29,  $-5.0$ , dash-dot line). The first two curves are models for dissociation of a singly protonated peptide along the oxazolone pathways initiated by migration of the extra proton at the N-terminus amino group and the final two are those for migration of the extra proton sequestered by the arginine side chain. (b) The internal energy distribution,  $P(E)$ , for the same protonated peptide calculated at 700 (solid line) and 1250 K (dashed line).

K using eqn. (2). The temperature was chosen such that the calculated  $k(E)$  results in dissociation of a substantial portion of the precursor ions. Use of different kinetic parameters, especially  $E_0$ , would result in different  $k(E)$ , which, in turn, would require different effective MALDI temperature. We repeated the calculations for various peptides with 5-15 amino acid residues using the same kinetic parameters and found that the efficient occurrence of PSD could be simulated through minor adjustment (around 50 K) of the effective temperature.

Before proceeding further, we checked our postulation of  $k_3 \gg k_{-2}$ . The critical energies for  $\text{C} \rightarrow \text{D} + \text{E}$  and  $\text{C} \rightarrow \text{B}$  were taken as 0.65 and 0.50 eV based on the potential energy diagram in Figure 1. Based on the expectation that the transition states for  $\text{C} \rightarrow \text{D} + \text{E}$  and  $\text{C} \rightarrow \text{B}$  would be loose and tight, respectively, 5 and  $-10$  eu were used as  $\Delta S^\ddagger$  for these steps. The results are shown in Figure 3. At the internal energy corresponding to the PSD range, the rate constant ( $k_3$ ) for  $\text{C} \rightarrow \text{D} + \text{E}$  is much larger than that ( $k_{-2}$ ) for  $\text{C} \rightarrow \text{B}$ . This is in agreement with our proposition that eqn. (5) is an adequate expression for the overall rate constant if the reaction in PSD occurs along the oxazolone pathway and if Figure 1 is a reasonable description of the potential energy along this pathway. Also to be noted in Figure 3 is that  $\text{B} \rightarrow \text{C}$  would not be rate-determining at very low internal energy range, *viz.* TS switching to  $\text{C} \rightarrow \text{D} + \text{E}$  may occur as mentioned above.

When the extra proton is sequestered by an arginine side chain, its migration to an amide nitrogen would require more energy than that of the proton attached at the amino group at the N-terminus in the absence of the arginine residue. Assuming that the protonated arginine residue did not interact with other parts of the protonated peptide,<sup>31</sup> we roughly estimated the stabilization of the global minimum in the presence of an arginine residue by utilizing the difference in proton affinity (PA) between arginine and other amino acids. Average PA of 19 amino acids other than

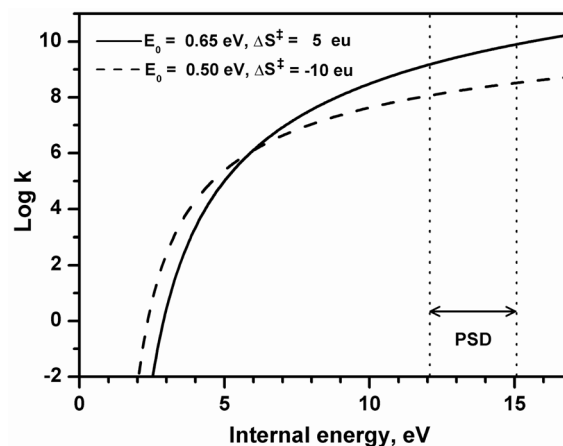


**Figure 3.** RRKM rate constants calculated with 1)  $E_0 = 0.65$  eV and  $\Delta S^\ddagger = 5$  eu and 2)  $E_0 = 0.50$  eV and  $\Delta S^\ddagger = -10$  eu are drawn as solid (—) and dashed (---) lines, respectively. 1) and 2) are models for  $k_3$  and  $k_{-2}$ , respectively. The internal energy range for PSD read from Fig. 2 is marked.

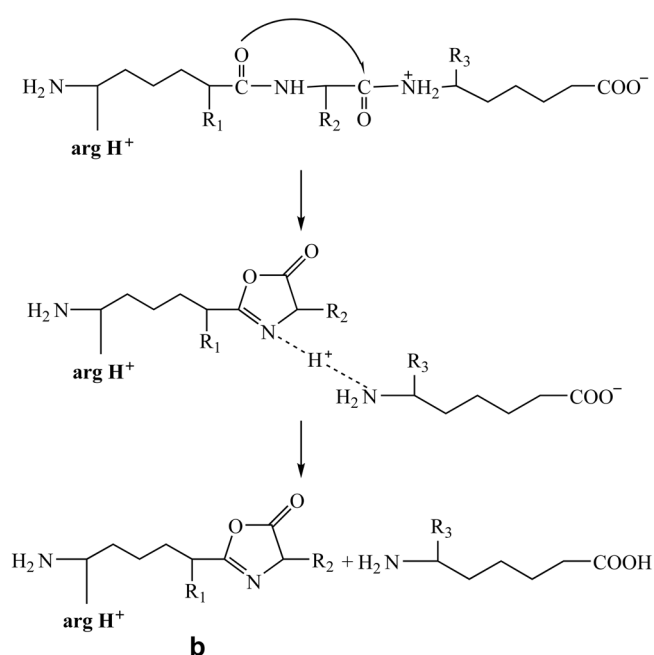
arginine was compared with PA of arginine. The PA differences of 1.07–1.20 eV were obtained depending on the PA data sets<sup>32–34</sup> used in the estimation. Based on this result, we will assume that sequestering of the extra proton by the arginine side chain lowers the energy of the global minimum by 1.1 eV compared to the structure with the extra proton attached to the amino group at the N-terminus. The situation is drawn in Figure 1. Let us suppose that the proton at the arginine side chain migrates to an amide nitrogen and that the remaining neutral arginine side chain does not interact with other parts in the protonated peptide. Then, the potential energy at  $TS_{BC}$  will become  $1.10 + 1.30 = 2.40$  eV. To see the effect of such an increase in the critical energy, we repeated  $k(E)$  calculation for  $[PKPQQFFGLMR+H]^+$  using  $E_0 = 2.40$  eV and  $\Delta S^\ddagger = 0$  eu. The result is also drawn in Figure 2(a).

It is to be noted from the figure that migration of the extra proton at the arginine side chain is quite unfavorable, reducing the rate constant by several orders of magnitude compared to the arginine-free case. Or, singly protonated peptides with an arginine residue requires 23 eV more internal energy for PSD than the arginine-free case. Based on the calculated  $P(E)$  curve shown in Figure 2(b), the effective MALDI temperature needed for the simultaneous observation of the singly protonated peptide and its PSD signals is around 1250 K when an arginine residue is present. The optimal MALDI condition is hardly affected by the peptide samples as far as the MALDI matrix and laser wavelength and focusing are kept the same. Then, the effective MALDI temperature for different samples would be very similar because it would be mostly determined by the laser and the matrix. That is, postulation of widely different effective MALDI temperature, 700 vs. 1250 K, for PSD of singly protonated peptides without and with an arginine residue looks entirely unrealistic. Many different sets of values for  $E_0$ ,  $\Delta S^\ddagger$ , and  $T$  other than 1.3 eV, 0.0 eu, and 700 K, respectively, are also compatible with strong appearance of PSD signals in the absence of arginine.  $k(E)$ s calculated with  $E_0 = 1.19$  eV and  $\Delta S^\ddagger = -5.0$  eu and with  $E_0 = 2.49$  eV and  $\Delta S^\ddagger = -5.0$  eu are also compared in Figure 2 to demonstrate that unrealistic results were obtained regardless of the parameter sets used.

Based on the results presented so far, it can be concluded that the migration of the extra proton sequestered at the arginine side chain followed by the dissociation along the oxazolone pathway is not a viable mechanism. In other pathways proposed for the formation of b- and/or y-type ions, *viz.* diketopiperazine and aziridone pathways,<sup>10,11</sup> facile migration of the extra proton is also presumed. They are not appropriate to handle the arginine case either.

## Discussion

As has been mentioned already, tandem mass spectra recorded under low internal energy regime are dominated by b- and/or y-type product ions even when an arginine residue is present in singly protonated peptides. In addition, b-type



**Scheme 2.** Oxazolone pathway initiated by migration of carboxyl proton.  $\text{argH}^+$  represents the arginine side chain which has sequestered the extra proton.

ions dominate when the arginine residue is at the N-terminus while y-type ions dominate when the same residue is at the C-terminus. That is, the overall spectral features look compatible with the oxazolone mechanism, even though the present work has found that the migration of the extra proton at the arginine side chain is highly unlikely. This suggests a possibility that a proton other than the one sequestered at the arginine side chain might migrate to an amide nitrogen followed by dissociation along the oxazolone pathway.

Even though amino acids and small peptides exist as zwitterions – let us use  $\text{NH}_3^+/\text{COO}^-$  to denote the protonation situation at the N- and C-termini – in the aqueous phase, normal forms (to be denoted as  $\text{NH}_2/\text{COOH}$ ) are known to be more stable in the gas phase.<sup>35–37</sup> When a peptide without a strongly basic residue is protonated, the structure at the global minimum would be  $\text{NH}_3^+/\text{COOH}$  as found by DFT calculations.<sup>11</sup> Assuming that the extra proton in a singly protonated peptide containing an arginine residue is sequestered by the arginine side chain, the tautomeric structure  $\text{NH}_2/\text{COOH}$  may be important. It is likely that the proton in  $\text{COOH}$  is easier to migrate than the proton sequestered at the arginine side chain. The oxazolone pathway initiated by migration of carboxyl proton for singly protonated peptides with an arginine residue at the N-terminus is drawn in Scheme 2. The deprotonated peptide in the proton-bound dimer would take the proton in this case, resulting in b-type ion as observed experimentally. A similar scheme can be drawn for singly protonated peptides with arginine at the C-terminus. In this case, y-type ions would be the major product ions.

If the carboxyl proton migration-oxazolone pathway is the answer to the arginine mystery, it should be possible to

quench the dissociation of singly protonated peptides with an arginine residue by eliminating the carboxyl proton through derivatization. Singly protonated substance P ( $[\text{RPKPQQFFGLM-NH}_2+\text{H}]^+$ ) is one of such cases. However, PSD spectrum of a singly protonated substance P can be recorded easily, even though the PSD efficiency measured by product: precursor ratio is not as good as for other singly protonated peptides with an arginine residue – PSD of  $[\text{PKPQQFFGLMR}+\text{H}]^+$  is two times more efficient than that of a singly protonated substance P. This suggests that the carboxyl proton migration-oxazolone pathway may not be an answer to the arginine mystery. Or, the mechanism may be valid even though other mechanisms may also operate.

It is to be noted that not only the global minimum structure but also the final products – such as y-type ions from singly protonated peptides with an arginine residue at the C-terminus – would be stabilized by sequestering of a proton. Then, dissociation of singly protonated peptides with an arginine residue will become efficient if the transition structure acting as the bottleneck such as  $\text{TS}_{\text{BC}}$  is also stabilized by arginine. That is, the arginine residue which has sequestered the extra proton may interact with other parts in the protonated peptide<sup>31</sup> all the way through the reaction path. Further experimental data are needed to see if dynamics of the dissociation of a singly protonated peptide occurring on a microsecond time scale would be affected by intramolecular interactions involving an arginine residue.

The kinetic analysis made so far suggests that  $E_0$  for dissociation of singly protonated peptides with arginine is larger than that in the arginine-free case, but only by a few tenths of an eV. In the surface-induced dissociation (SID) study reported by Wysocki *et al.*,<sup>8</sup> the fragmentation efficiency curves (drawn as functions of collision energy) for protonated peptides with and without a mobile proton – which may correspond to singly protonated peptides without and with an arginine residue, respectively – were well separated. This suggested that the dissociation of the latter ions required substantially more energy than those for the former ions. Then, the question is whether the slight difference in the critical energy between the two cases indicated in our kinetic study would be large enough to display noticeable difference in the SID data. As an effort to find an answer to this question, we performed  $k(E)$  calculation (not shown) using  $E_0 = 1.5$  eV which higher by 0.2 eV than 1.3 eV used in the previous calculation. It was found that the average internal energy needed for PSD at  $E_0 = 1.5$  eV was larger than that at  $E_0 = 1.3$  eV by 3.5 eV. That is, even though the difference in  $E_0$  between the two cases is small, the corresponding difference in internal energy is much larger because of the large kinetic shift<sup>38</sup> associated with the dissociation of large molecules. Since only a fraction of collision energy would be converted to internal energy in SID, the fragmentation efficiency curves drawn as functions of collision energy for protonated peptides with and without an arginine residue, or without and with a mobile proton, would appear well separated as observed experimentally. That is, our finding that  $E_0$  values in the dissociation of

protonated peptides with and without arginine are only slightly different is not contradictory with good separation of their SID efficiency curves. This, in turn, suggests that dissociation of singly protonated peptides with arginine does not occur along the original oxazolone pathway as claimed in this work.

## Conclusion

It is widely thought that b- and y-type fragment ions are formed from protonated peptides without arginine mainly *via* a multi-step process called the oxazolone pathway. In this work, a simple kinetic model has been derived for such reactions occurring on a microsecond time scale through kinetic arguments and computations. The model has been used to probe whether this pathway is also applicable to singly protonated peptide with an arginine residue and, if it is applicable, whether the extra proton sequestered by arginine will migrate to an amide nitrogen where charge-directed dissociation is thought to occur. It has been found that migration of the extra proton is highly unlikely. Regardless, it is known that b- and y-type ions are the main product ions even when arginine is present and that b-or-y branching is determined in the same way as in the arginine-free cases, suggesting that protonated peptides with arginine may dissociate *via* a mechanism resembling the original oxazolone pathway. If such a mechanism exists, a requirement would be facile migration of a proton, not the extra proton sequestered at arginine but a proton at somewhere else, to an amide nitrogen. We do not know at the moment how dissociation of protonated peptides with arginine proceeds, even though some possibilities have been mentioned. It is acknowledged that the kinetic treatment made in this work is gross in nature and the parameters used are probably inaccurate. More elaborate experimental and theoretical efforts are needed to solve this arginine mystery, especially because the subject is relevant to developing new techniques for protein analysis.

**Acknowledgments.** This work was financially supported by Korea Research Foundation, Republic of Korea and by the Bio-signal Analysis Technology Innovation program (M10645010002-06N4501-00210) of the Ministry of Education and Science, Republic of Korea. Y. J. Chung and S. H. Yoon thank the Ministry of Education and Science, Republic of Korea, for Brain Korea 21 Fellowship.

## References

1. Mann, M.; Hendrickson, R. C.; Pandey, A. *Annu. Rev. Biochem.* **2001**, *70*, 437.
2. Kinter, M.; Sherman, N. E. *Protein Sequencing and Identification Using Tandem Mass Spectrometry*; Desiderio, D. M.; Nibbering, N. M. M., Eds.; John Wiley: New York, U. S. A., 2005.
3. Hernandez, P.; Müller, M.; Appel, R. D. *Mass Spectrom. Rev.* **2006**, *25*, 235.
4. Yoon, T. O.; Choi, C. M.; Kim, H. J.; Kim, N. J. *Bull. Korean Chem. Soc.* **2007**, *28*, 619.
5. Cotter, R. J. *Time-of-Flight Mass Spectrometry*; ACS: Washington, U. S. A., 1997; p 237.

6. Cole, R. B. *Electrospray Ionization Mass Spectrometry*; Wiley-Interscience: New York, 1997.
  7. Hillenkamp, F.; Karas, M.; Beavis, R. C.; Chait, B. T. *Anal. Chem.* **1991**, *63*, 1193A.
  8. Wysocki, V. H.; Tsapraillis, G.; Smith, L. L.; Brechi, L. A. *J. Mass Spectrom.* **2000**, *35*, 1399.
  9. Summerfield, S. G.; Whiting, A.; Gaskell, S. J. *Int. J. Mass Spectrom. Ion Processes* **1997**, *162*, 149.
  10. Rodriguez, C. F.; Cunje, A.; Shoeib, T.; Chu, I. K.; Hopkinson, A. C.; Siu, K. W. M. *J. Am. Chem. Soc.* **2001**, *123*, 3006.
  11. Paizs, B.; Suhai, S. *Rapid Commun. Mass Spectrom.* **2002**, *16*, 375.
  12. Paizs, B.; Suhai, S. *J. Am. Soc. Mass Spectrom.* **2004**, *15*, 103.
  13. Paizs, B.; Suhai, S. *Mass Spectrom. Rev.* **2005**, *24*, 508.
  14. Polce, M. J.; Ren, D.; Wesdemiotis, C. *J. Mass Spectrom.* **2000**, *35*, 1391.
  15. Cox, K. A.; Gaskell, S. J.; Morris, M.; Whiting, A. *J. Am. Soc. Mass Spectrom.* **1996**, *7*, 522.
  16. Yoon, S. H.; Kim, M. S. *J. Am. Soc. Mass Spectrom.* **2007**, *18*, 1729.
  17. Yoon, S. H.; Chung, Y. J.; Kim, M. S. *J. Am. Soc. Mass Spectrom.* **2008**, *19*, 645.
  18. Robinson, P. J.; Holbrook, K. A. *Unimolecular Reactions*; Wiley Interscience: New-York, 1972; p 52.
  19. Rosenstock, H. M.; Wallenstein, M. B.; Wahrhaftig, A. L.; Eyring, H. *Proc. Natl. Acad. Sci. U.S.A.* **1952**, *38*, 667.
  20. Baer, T.; Hase, W. L. *Unimolecular Reaction Dynamics: Theory and Experiments*; Oxford Univ. Press: New York, 1996; p 171.
  21. Moon, J. H.; Oh, J. Y.; Kim, M. S. *J. Am. Soc. Mass Spectrom.* **2006**, *17*, 1749.
  22. Moon, J. H.; Sun, M.; Kim, M. S. *J. Am. Soc. Mass Spectrom.* **2007**, *18*, 1063.
  23. Sun, M.; Moon, J. H.; Kim, M. S. *J. Phys. Chem. B* **2007**, *111*, 2747.
  24. Holbrook, K. A.; Pilling, M. J.; Robertson, S. H. *Unimolecular Reactions*, 2nd ed.; Wiley: Chichester, UK, 1996.
  25. Lifshitz, C. *Adv. Mass Spectrom.* **1989**, *11A*, 713.
  26. Beyer, T.; Swinehart, D. F. *Commun. ACM* **1973**, *16*, 379.
  27. Baer, T.; Hase, W. L. *Unimolecular Reaction Dynamics: Theory and Experiments*; Oxford Univ. Press: New York, 1996; p 272.
  28. Laskin, J.; Denisov, E.; Futrell, J. H. *Int. J. Mass Spectrom.* **2002**, *219*, 189.
  29. Johnson, R. S.; Martin, S. A.; Biemann, K. *Int. J. Mass Spectrom. Ion Processes* **1988**, *86*, 137.
  30. Bythell, B. J.; Barofsky, D. F.; Pingitore, F.; Polce, M. J.; Wang, P.; Wesdemiotis, C.; Paizs, B. *J. Am. Soc. Mass Spectrom.* **2007**, *18*, 1921.
  31. Wyttenbach, T.; von Helden, G.; Bowers, M. T. *J. Am. Chem. Soc.* **1996**, *118*, 8355.
  32. Lias, S. G.; Liebman, J. F.; Levin, R. D. *J. Phys. Chem. Ref. Data* **1984**, *13*, 695.
  33. Harrison, A. G. *Mass Spectrom. Rev.* **1997**, *16*, 201.
  34. Maksiaë, Z. B.; Kovaëviaë, B. *Chem. Phys. Lett.* **1999**, *307*, 497.
  35. Vishveshwara, S.; Pople, J. A. *J. Am. Chem. Soc.* **1977**, *99*, 2422.
  36. Suenram, R. D.; Lovas, F. J. *J. Mol. Spectrosc.* **1978**, *72*, 372.
  37. Kang, Y. K.; Byun, B. J.; Kim, Y. H.; Kim, Y. H.; Lee, D. H.; Lee, J. Y. *Bull. Korean Chem. Soc.* **2008**, *29*, 1149.
  38. Lifshitz, C. *Mass Spectrom. Rev.* **1982**, *1*, 309.
-